

A Homologous Series of Alkaline Earth Phosphanides: Syntheses, Crystal Structures, and Unusual Dynamic Behavior of $(\text{THF})_n\text{M}[\text{P}\{\text{CH}(\text{SiMe}_3)_2\}(\text{C}_6\text{H}_4\text{-2-CH}_2\text{NMe}_2)]_2$ ($\text{M} = \text{Mg, Ca, Sr, Ba}$)

Stuart Blair, Keith Izod,* and William Clegg

Department of Chemistry, Bedson Building, University of Newcastle, Newcastle upon Tyne NE1 7RU, U.K.

Received February 11, 2002

The secondary phosphine $\text{R}(\text{Me}_2\text{NCH}_2\text{-2-C}_6\text{H}_4)\text{PH}$ reacts with Bu_2Mg to give the homoleptic complex $\text{Mg}\{\text{PR}(\text{C}_6\text{H}_4\text{-2-CH}_2\text{NMe}_2)_2\}_2$ (**1**) [$\text{R} = \text{CH}(\text{SiMe}_3)_2$]. The analogous heavier alkaline earth metal complexes $(\text{THF})_n\text{Ae}\{\text{PR}(\text{C}_6\text{H}_4\text{-2-CH}_2\text{NMe}_2)_2\}_2$ [$\text{Ae} = \text{Ca}$ (**2**), $n = 0$; $\text{Ae} = \text{Sr}$ (**3**), Ba (**4**), $n = 1$] have been synthesized by metathesis reactions between $\text{K}\{\text{PR}(\text{C}_6\text{H}_4\text{-2-CH}_2\text{NMe}_2)\}$ and 0.5 equiv of the respective alkaline earth metal diiodide. Compounds **1–4** have been characterized by X-ray crystallography and multielement NMR spectroscopy. In the solid state, compounds **1–4** are monomeric, complexes **1** and **2** adopting a distorted tetrahedral geometry and complexes **3** and **4** adopting a distorted square pyramidal geometry (**1**: orthorhombic, $P2_12_12_1$, $a = 11.413(3)$ Å, $b = 12.072(3)$ Å, $c = 32.620(11)$ Å, $Z = 4$. **2**: monoclinic, $P2_1/c$, $a = 9.5550(4)$ Å, $b = 17.4560(7)$ Å, $c = 24.5782(10)$ Å, $\beta = 91.673(2)^\circ$, $Z = 4$. **3**: monoclinic, $C2/c$, $a = 15.0498(9)$ Å, $b = 13.0180(8)$ Å, $c = 24.3664(14)$ Å, $\beta = 104.593(2)^\circ$, $Z = 4$. **4**: monoclinic, $C2/c$, $a = 15.2930(10)$ Å, $b = 13.0326(9)$ Å, $c = 24.6491(17)$ Å, $\beta = 105.542(2)^\circ$, $Z = 4$). In toluene solution, compounds **2–4** are subject to dynamic processes which are attributed to a monomer–dimer equilibrium for which bridge–terminal exchange of the phosphanide ligands in the dimer may be frozen out at low temperatures.

Introduction

Complexes of the heavier alkaline earth metal cations (Ca^{2+} , Sr^{2+} , Ba^{2+}) exhibit a pronounced tendency toward aggregation and/or solvation by neutral donor molecules because of their extremely large ionic radii.¹ Thus, the synthesis of molecular complexes of these elements with ligands such as alkoxides, amides, and hydrocarbyls requires the use of sterically demanding groups which block vacant coordination sites and hence prevent oligomerization to form extended polymers or 3-dimensional arrays. Nevertheless, the tendency toward oligomerization is increased for the lower members of the group. In this context, the bis(trimethylsilyl)amides of the group 2 elements form an interesting homologous series: in the absence of donor solvents, the bis(trimethylsilyl)amides of Mg, Ca, Sr, and Ba adopt an identical structural motif in the solid state; all

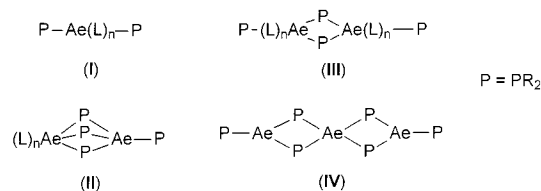
four complexes adopt dimeric structures of the form $[\{(\text{Me}_3\text{-Si})_2\text{N}\}\text{Ae}\{\mu\text{-N}(\text{SiMe}_3)_2\}_2\text{Ae}\{\text{N}(\text{SiMe}_3)_2\}]_2$, despite the large variation in ionic radii of the group 2 cations.² In the presence of donor solvents such as THF, the alkaline earth bis(trimethylsilyl)amides crystallize as solvated monomers of the form $(\text{L})_n\text{Ae}\{\text{N}(\text{SiMe}_3)_2\}_2$.^{2a} In contrast, the bis(trialkylsilyl)phosphanides of the group 2 elements exhibit a greater diversity of structures in the solid state.³ X-ray crystallography reveals that alkaline earth bis(trialkylsilyl)phosphanide complexes typically adopt one of three structural types in the solid state: (i) solvated monomers, for example, $\{(\text{Me}_3\text{Si})_2\text{P}\}_2\text{Ca}(\text{THF})_4$ (**I**),^{3a} (ii) unsymmetrical dimers, for example, $\{(\text{Me}_3\text{Si})_2\text{P}\}\text{Sr}\{\mu\text{-P}(\text{SiMe}_3)_2\}_3\text{Sr}(\text{THF})_3$ (**II**),^{3b} and (iii) symmetrical dimers, for example, $[(\text{THF})_2\{(\text{Me}_2\text{Pr}^i\text{-Si})_2\text{P}\}_2\text{Ba}]_2$ (**III**),^{3c} although linear trimers, for example,

(2) Westerhausen, M. *Coord. Chem. Rev.* **1998**, *176*, 157. (b) Westerhausen, M.; Schwarz, W. *Z. Anorg. Allg. Chem.* **1992**, *609*, 39. (c) Westerhausen, M.; Schwarz, W. *Z. Anorg. Allg. Chem.* **1991**, *604*, 127. (d) Westerhausen, M.; Schwarz, W. *Z. Anorg. Allg. Chem.* **1991**, *606*, 177. (e) Vaartsrta, B. A.; Huffmann, J. C.; Streib, W. E.; Caulton, K. G. *Inorg. Chem.* **1991**, *30*, 121.

* To whom correspondence should be addressed. E-mail: k.j.izod@ncl.ac.uk.

(1) Hanusa, T. *P. Chem. Rev.* **1993**, *93*, 1023.

$\{[(\text{Me}_3\text{Si})_2\text{P}]\text{Mg}\{\mu\text{-P}(\text{SiMe}_3)_2\}_2\}_2\text{Mg}$ (IV),^{3d} have also been observed.



In addition to these structural types, tetramers and hexamers have been isolated with doubly charged phosphinediide ligands, RP^{2-} ,^{3m,4} and a number of mixed metal clusters containing these ligands have been reported.^{5,3a}

Almost without exception, phosphanide complexes of the heavier alkaline earths (Ca, Sr, and Ba) are limited to ligands which have silicon-containing substituents directly bonded to the phosphorus donor atom, $(\text{R}_3\text{Si})\text{R}'\text{P}^-$ [R_3Si = for example, Me_3Si , $\text{Me}_2\text{Pr}^i\text{Si}$, Pr^i_3Si ; $\text{R}' = \text{H}$, R_3Si], in which the silyl substituents assist in the steric saturation of the metal centers, preventing extensive oligomerization and stabilizing the complex toward nucleophilic attack.³ For Be and Mg, such stabilization is more easily achieved, and molecular complexes containing quite simple alkyl- or aryl-substituted phosphanide ligands have been isolated [for example, $(\text{tmeda})\text{Mg}(\text{P}(\text{HPh})_2)$].^{3k,6}

We recently reported the synthesis and structural characterization of a novel calcium alkoxo-phosphanide heterocubane cluster, generated by an unusual ligand cleavage reaction.⁷ This cluster contains a dianionic ligand $\{[(\text{Me}_3\text{Si})_2\text{CH}]\text{P}(\text{C}_6\text{H}_4\text{-}2\text{-O})\}^{2-}$, in which the phosphorus donor atom is not directly bonded to silyl substituents, the first time that such a complex had been isolated for a heavier alkaline earth metal. We now describe the synthesis, structural characterization, and solution behavior of a homologous series of

alkaline earth metal phosphanides, $(\text{THF})_n\text{Ae}\{[\text{P}\{\text{CH}(\text{SiMe}_3)_2\}(\text{C}_6\text{H}_4\text{-}2\text{-CH}_2\text{NMe}_2)]_2\}$ [$\text{Ae} = \text{Mg}$, Ca , $n = 0$; $\text{Ae} = \text{Sr}$, Ba , $n = 1$], bearing a related, monoanionic ligand.

Experimental Section

General. All manipulations were carried out using standard Schlenk techniques under an atmosphere of dry nitrogen. Ether, THF, and light petroleum (bp 40–60 °C) were distilled from potassium or sodium/potassium alloy, and hexamethyldisiloxane was distilled from CaH_2 , under an atmosphere of dry nitrogen. These were stored over a potassium film (except THF and hexamethyldisiloxane, which were stored over activated 4 Å molecular sieves). Deuterated toluene was distilled from potassium and deoxygenated by three freeze–pump–thaw cycles and was stored over activated 4 Å molecular sieves. Bu_2Mg was purchased from Aldrich as a 1.0 M solution in heptane. CaI_2 , SrI_2 , and BaI_2 were purchased from Aldrich or Strem as anhydrous solids and were used without further purification. $\{(\text{Me}_3\text{Si})_2\text{CH}\}\{\text{C}_6\text{H}_4\text{-}2\text{-CH}_2\text{NMe}_2\}\text{PH}$ and $\{[(\text{Me}_3\text{Si})_2\text{CH}]\{\text{C}_6\text{H}_4\text{-}2\text{-CH}_2\text{NMe}_2\}\text{PK}$ were prepared according to previously published procedures.⁸

³¹P NMR spectra were recorded on a Bruker WM300 spectrometer operating at 121.5 MHz, and ¹H and ¹³C spectra were recorded on a Bruker AC200 spectrometer operating at 200.1 and 50.3 MHz, respectively. ¹H and ¹³C chemical shifts are quoted in ppm relative to tetramethylsilane; ³¹P chemical shifts are quoted relative to external 85% H_3PO_4 . Elemental analyses were obtained by Elemental Microanalysis Ltd., Okehampton, U.K.; because of the extreme air sensitivity of **1–4**, reproducible CHN analyses were not always obtained.

Preparation of $\text{Mg}\{[\text{P}\{\text{CH}(\text{SiMe}_3)_2\}\{\text{C}_6\text{H}_4\text{-}2\text{-CH}_2\text{NMe}_2\}]_2$ (1). To a solution of $\{[(\text{Me}_3\text{Si})_2\text{CH}]\{\text{C}_6\text{H}_4\text{-}2\text{-CH}_2\text{NMe}_2\}\text{PH}$ (0.46 g, 1.41 mmol) in light petroleum (10 mL) was added Bu_2Mg (0.71 mL, 0.71 mmol), and the pale yellow solution was stirred for 16 h. Solvent was removed in vacuo, and the product was extracted into hexamethyldisiloxane (10 mL) and filtered. After standing at room temperature for 16 h, the pale yellow crystalline solid was isolated and recrystallized from cold (5 °C) hexamethyldisiloxane/THF (5 mL/0.5 mL) as pale yellow needles of **1**·THF. Yield 0.23 g, 48%. Anal. Calcd for $\text{C}_{32}\text{H}_{62}\text{MgN}_2\text{P}_2\text{Si}_4$ (molecular formula without solvent of crystallization): C, 57.07; H, 9.28; N, 4.16. Found: C, 55.55; H, 9.72; N, 3.87. ¹H NMR (*d*₈-THF): $\delta = 0.15$ (s, 18H, SiMe₃), 0.41 (s, 18H, SiMe₃), 0.66 (s, 6H, NMe₂), 0.77 (s, 2H, CHP), 1.99 (s, 6H, NMe₂), 2.20 [d, ²J_{HH} = 9.9 Hz, 2H, CH₂N], 4.13 [d, ²J_{HH} = 9.9 Hz, 2H, CH₂N], 6.38 (m, 2H, ArH), 6.53 (m, 2H, ArH), 6.96 (m, 2H, ArH), 7.27 (m, 2H, ArH). ¹³C{¹H} NMR (*d*₈-toluene): $\delta = 1.31$ (SiMe₃), 2.03 (SiMe₃), 5.41 [d, $J_{\text{PC}} = 42.3$ Hz, CHP], 43.06, 45.70 (NMe₂), 64.72 [d, $J_{\text{PC}} = 25.9$ Hz, CH₂N], 118.31 (aryl), 129.06, 129.36 (aryl), 131.73 [d, $J_{\text{PC}} = 23.7$ Hz, aryl], 136.50 (aryl), 154.56 [d, $J_{\text{PC}} = 48.5$ Hz, aryl]. ³¹P{¹H} NMR (*d*₈-toluene): $\delta = -96.8$.

Preparation of $\text{Ca}\{[\text{P}\{\text{CH}(\text{SiMe}_3)_2\}\{\text{C}_6\text{H}_4\text{-}2\text{-CH}_2\text{NMe}_2\}]_2$ (2). To a suspension of CaI_2 (0.25 g, 0.84 mmol) in THF (5 mL) was added, dropwise, a solution of $\{[(\text{Me}_3\text{Si})_2\text{CH}]\{\text{C}_6\text{H}_4\text{-}2\text{-CH}_2\text{NMe}_2\}\text{PK}$ (0.66 g, 1.69 mmol) in THF (15 mL). The mixture was allowed to stir for 16 h, and then solvent was removed in vacuo. The residue was extracted into ether (20 mL) and filtered. Solvent was removed from the filtrate in vacuo, and the sticky yellow material was washed with hexamethyldisiloxane (2 × 15 mL) to give a yellow solid. This was recrystallized from cold (5 °C) ether

- (3) (a) Westerhausen, M.; Schwarz, W. *Z. Anorg. Allg. Chem.* **1996**, 622, 903. (b) Westerhausen, M. *J. Organomet. Chem.* **1994**, 479, 141. (c) Westerhausen, M.; Lang, G.; Schwarz, W. *Chem. Ber.* **1996**, 129, 1035. (d) Westerhausen, M.; Digeser, M. H.; Wieneke, B.; Nöth, H.; Knizek, J. *Eur. J. Inorg. Chem.* **1998**, 517. (e) Westerhausen, M.; Hartmann, M.; Schwarz, W. *Inorg. Chem.* **1996**, 35, 2421. (f) Westerhausen, M.; Low, R.; Schwarz, W. *J. Organomet. Chem.* **1996**, 513, 213. (g) Westerhausen, M.; Schwarz, W. *J. Organomet. Chem.* **1993**, 463, 51. (h) Westerhausen, M.; Digeser, M. H.; Noth, H.; Knizek, J. *Z. Anorg. Allg. Chem.* **1998**, 624, 215. (i) Westerhausen, M.; Schwarz, W. *Z. Anorg. Allg. Chem.* **1994**, 620, 304. (j) Westerhausen, M.; Pfitzner, A. *J. Organomet. Chem.* **1995**, 487, 187. (k) Hey, E.; Engelhardt, L. M.; Raston, C. L.; White, A. H. *Angew. Chem., Int. Ed. Engl.* **1987**, 26, 81. (l) Westerhausen, M.; Digeser, M.; Krofta, M.; Wiberg, N.; Noth, H.; Knizek, J.; Ponikwar, W.; Seifert, T. *Eur. J. Inorg. Chem.* **1999**, 743. (m) Westerhausen, M.; Krofta, M.; Mayer, P. *Z. Anorg. Allg. Chem.* **2000**, 626, 2307. (n) Westerhausen, M.; Digeser, M. H.; Noth, H.; Ponikwar, W.; Seifert, T.; Polborn, K. *Inorg. Chem.* **1999**, 38, 3207.
- (4) (a) Westerhausen, M.; Krofta, M.; Pfitzner, A. *Inorg. Chem.* **1999**, 38, 598. (b) Westerhausen, M.; Krofta, M.; Mayer, P.; Warchhold, M.; Noth, H. *Inorg. Chem.* **2000**, 39, 4721. (c) Westerhausen, M.; Schneiderbauer, S.; Knizek, J.; Noth, H.; Pfitzner, A. *Eur. J. Inorg. Chem.* **1999**, 2215. (d) Westerhausen, M.; Birg, C.; Krofta, M.; Mayer, P.; Seifert, T.; Noth, H.; Pfitzner, A.; Nilges, T.; Deiseroth, H.-J. *Z. Anorg. Allg. Chem.* **2000**, 626, 1073.
- (5) (a) Westerhausen, M.; Hausen, H.-D.; Schwarz, W. *Z. Anorg. Allg. Chem.* **1995**, 621, 877. (b) Westerhausen, M.; Enzelberger, M. M.; Schwarz, W. *J. Organomet. Chem.* **1995**, 491, 83.
- (6) Atwood, J. L.; Bott, S. G.; Jones, R. A.; Koschmieder, S. U. *Chem. Commun.* **1990**, 692.
- (7) Izod, K.; Clegg, W.; Liddle, S. T. *Organometallics*, **2000**, 19, 3640.

- (8) Clegg, W.; Doherty, S.; Izod, K.; Kagerer, H.; O'Shaughnessy, P.; Sheffield, J. M. *J. Chem. Soc., Dalton Trans.* **1999**, 1825.

Table 1. Crystallographic Data for 1–4

| | 1 | 2 | 3 | 4 |
|--|--|---|---|--|
| formula | C ₃₂ H ₆₂ MgN ₂ P ₂ Si ₄ .C ₄ H ₈ O | C ₃₂ H ₆₂ CaN ₂ P ₂ Si ₄ | C ₃₆ H ₇₀ N ₂ OP ₂ Si ₄ Sr | C ₃₆ H ₇₀ BaN ₂ OP ₂ Si ₄ |
| fw | 745.55 | 689.22 | 808.86 | 858.58 |
| cryst syst | orthorhombic | monoclinic | monoclinic | monoclinic |
| space group | <i>P</i> 2 ₁ 2 ₁ 2 ₁ | <i>P</i> 2 ₁ / <i>c</i> | <i>C</i> 2/ <i>c</i> | <i>C</i> 2/ <i>c</i> |
| <i>a</i> , Å | 11.413(3) | 9.5550(4) | 15.0498(9) | 15.2930(10) |
| <i>b</i> , Å | 12.072(3) | 17.4560(7) | 13.0180(8) | 13.0326(9) |
| <i>c</i> , Å | 32.620(11) | 24.5782(10) | 24.3664(14) | 24.6491(17) |
| β , deg. | 90 | 91.673(2) | 104.593(2) | 105.542(2) |
| <i>V</i> , Å ³ | 4495(2) | 4097.7(3) | 4619.8(5) | 4733.1(6) |
| <i>Z</i> | 4 | 4 | 4 | 4 |
| ρ_{calcd} , g cm ⁻³ | 1.102 | 1.117 | 1.163 | 1.205 |
| μ , mm ⁻¹ | 0.245 | 0.371 | 1.367 | 1.034 |
| <i>T</i> , K | 160 | 160 | 160 | 160 |
| <i>R</i> , <i>R</i> _w ^a (<i>F</i> ² > 2 σ) | 0.0411, 0.0903 | 0.0379, 0.0937 | 0.0382, 0.0925 | 0.0632, 0.1412 |
| <i>R</i> , <i>R</i> _w ^a (all data) | 0.0692, 0.0988 | 0.0526, 0.1012 | 0.0512, 0.0978 | 0.0985, 0.1609 |
| <i>S</i> ^a | 1.040 | 1.062 | 1.041 | 1.079 |
| data/parameters | 10677, 431 | 9539, 386 | 5459, 218 | 5691, 227 |

^a Conventional $R = \sum ||F_o| - |F_c|| / \sum |F_o|$; $R_w = [\sum w(F_o^2 - F_c^2)^2 / \sum w(F_o^2)^2]^{1/2}$; $S = [\sum w(F_o^2 - F_c^2)^2 / (\text{no. data} - \text{no. params})]^{1/2}$ for all data.

(~10 mL) as yellow blocks of **2**. Yield 0.42 g, 72%. Anal. Calcd for C₃₂H₆₂CaN₂P₂Si₄: C, 55.77; H, 9.07; N, 4.06. Found: C, 53.90; H, 9.51; N, 3.61. ¹H NMR (*d*₈-toluene): $\delta = 0.15$ (s, br, 18H, SiMe₃), 0.35 (s, br, 18H, SiMe₃), 0.64 (s, br, 2H, CHP), 0.91 (s, br, 6H, NMe₂), 1.84 (s, br, 6H, NMe₂), 2.23 (s, br, 2H, CH₂N), 4.02 (s, br, 2H, CH₂N), 6.35 (m, br, 2H, ArH), 6.40 (m, br, 2H, ArH), 6.84 (m, br, 2H, ArH), 7.23 (m, br, 2H, ArH). ¹³C{¹H} NMR (*d*₈-toluene): $\delta = 0.44$ (br, SiMe₃), 1.89 (br, SiMe₃), 4.85 [d, *J*_{PC} = 66.1 Hz, CHP], 40.31, 44.00 (br, NMe₂), 64.22 [d, *J*_{PC} = 25.9 Hz, CH₂N], 117.06, 129.01 (aryl), 130.20 [d, *J*_{PC} = 25.9 Hz, aryl], 131.18 (aryl), 157.37 [d, *J*_{PC} = 65.1 Hz, aryl]. ³¹P{¹H} NMR (*d*₈-toluene): $\delta = -70.7$.

Preparation of (THF)Sr[P{CH(SiMe₃)₂}{C₆H₄-2-CH₂NMe₂}]₂ (3**).** To a suspension of SrI₂ (0.34 g, 1.00 mmol) in THF (5 mL) was added, dropwise, a solution of [(Me₃Si)₂CH]{C₆H₄-2-CH₂-NMe₂}P]K (0.64 g, 2.00 mmol) in THF (20 mL), and the mixture was stirred for 16 h. Solvent was removed in vacuo, and the residue was extracted into ether (20 mL) and filtered. Solvent was removed in vacuo from the filtrate, and the residue was washed with hexamethyldisiloxane (2 × 15 mL) to leave a yellow solid. Recrystallization from ether (~10 mL) at 5 °C gave **3** as yellow blocks. Yield 0.44 g, 54%. Anal. Calcd for C₃₆H₇₀N₂OP₂Si₄Sr: C, 53.46; H, 8.72; N, 3.46. Found: C, 51.92; H, 8.79; N, 4.06. ¹H NMR (*d*₈-toluene): $\delta = 0.18$ (s, br, 36H, SiMe₃), 0.60 (s, 2H, CHP), 1.35 (m, 4H, THF), 1.81 (s, br, 12H, NMe₂), 2.50 (s, br, 2H, CH₂N), 3.50 (m, 4H, THF), 3.90 (s, br, 2H, CH₂N), 6.41 (m, br, 2H, ArH), 6.46 (m, br, 2H, ArH), 6.83 (t, br, 2H, ArH), 7.20 (d, br, 2H, ArH). ¹³C{¹H} NMR (*d*₈-toluene): $\delta = 0.44$ (br, SiMe₃), 5.40 (br, CHP), 42.56 (br, NMe₂), 65.80 (br, CH₂N), 116.99, 131.43, 131.96, 132.24, 159.98 (aryl). ³¹P{¹H} NMR (*d*₈-toluene): $\delta = -61.5$.

Preparation of (THF)Ba[P{CH(SiMe₃)₂}{C₆H₄-2-CH₂NMe₂}]₂ (4**).** To a suspension of BaI₂ (0.24 g, 0.60 mmol) in THF (5 mL) was added, dropwise, a solution of [(Me₃Si)₂CH]{C₆H₄-2-CH₂-NMe₂}P]K (0.47 g, 1.20 mmol) in THF (15 mL). The solution was left to stir for 16 h, and then, solvent was removed in vacuo, and the residue was extracted into ether (20 mL). The solution was concentrated to ca. 5 mL and cooled to 5 °C for 24 h, yielding **4** as orange blocks. Yield 0.32 g, 62%. Anal. Calcd for C₃₆H₇₀N₂OP₂Si₄Ba: C, 50.36; H, 8.22; N, 3.26. Found: C, 48.43; H, 8.54; N, 3.26. ¹H NMR (*d*₈-toluene): $\delta = 0.20$ (s, br, 36H, SiMe₃), 0.55 (s, 2H, CHP), 1.34 (m, 4H, THF), 1.77 (s, br, 12H, NMe₂), 2.50 (s, br, 2H, CH₂N), 3.44 (m, 4H, THF), 3.80 (m, br, 2H, CH₂N), 6.35 (m, br, 2H, ArH), 6.45 (s, br, 2H, ArH), 6.76 (m, br, 2H, ArH), 7.10 (m, br, 2H, ArH). ¹³C{¹H} NMR (*d*₈-toluene): $\delta =$

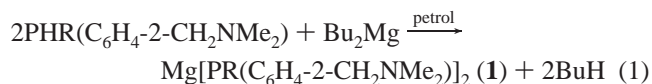
1.22 (br, SiMe₃), 6.88 [d, *J*_{PC} = 69.2 Hz, CHP], 42.95 (br, NMe₂), 64.35 [d, *J*_{PC} = 26.8 Hz, CH₂N], 115.50 (aryl), 129.50 [d, *J*_{PC} = 26.9 Hz, aryl], 131.64 (aryl), 162.73 [d, *J*_{PC} = 73.4 Hz, aryl]. ³¹P{¹H} NMR (*d*₈-toluene): $\delta = -42.5$.

X-ray Data Collection, Structure Determination and Refinement for 1–4. Crystal data are given in Table 1, and further details of the structure determinations are in the Supporting Information. Crystals were examined on a Bruker AXS CCD area-detector diffractometer with Mo K α radiation ($\lambda = 0.71073$ Å). Intensities were integrated from more than a hemisphere of data recorded on 0.3° frames by ω rotation. Semiempirical absorption corrections were applied, based on symmetry-equivalent and repeated data.

The structures were solved variously by direct and heavy-atom methods and were refined by least-squares methods on all unique *F*² values, with anisotropic displacement parameters, and with constrained riding hydrogen atoms. Two-fold disorder of coordinated THF on a crystallographic *C*₂ axis was successfully resolved in **3** and **4**. Programs were standard Bruker AXS control and integration software and SHELXTL (Bruker AXS Inc., Madison, WI). Complete results can be found in the Supporting Information.

Results and Discussion

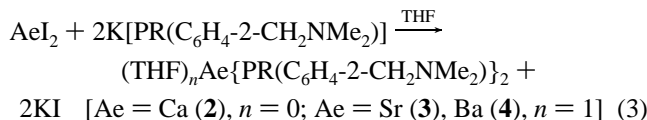
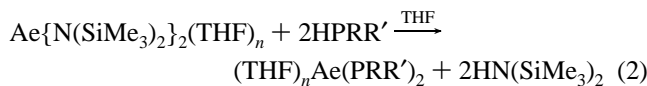
The reaction between dibutylmagnesium and the secondary phosphine PHR(C₆H₄-2-CH₂NMe₂) in light petroleum proceeds cleanly to give the highly air and moisture sensitive magnesium bis(phosphanide) Mg[PR(C₆H₄-2-CH₂NMe₂)]₂ (**1**) in satisfactory yield [R = CH(SiMe₃)₂] (eq 1).



Compound **1** is very soluble in hydrocarbon and ethereal solvents but may be recrystallized as pale yellow needles from the extremely poor solvent hexamethyldisiloxane.

The lack of conveniently accessible organo-calcium, -strontium, or -barium precursors precludes the use of this route for the synthesis of complexes containing these elements. Typically, heavier alkaline earth metal phosphanides have been synthesized via protonation of the corresponding alkaline earth metal amide by a primary or secondary phosphine (eq 2).² We have found that a straightforward metathesis reaction between 2 equiv of the readily

accessible potassium phosphanide $K\{PR(C_6H_4-2-CH_2NMe_2)\}$ and the respective alkaline earth metal diiodide in THF gives the compounds $(THF)_n Ae\{PR(C_6H_4-2-CH_2NMe_2)\}_2$ [$Ae = Ca$ (**2**), $n = 0$; $Ae = Sr$ (**3**), Ba (**4**), $n = 1$] as highly air-sensitive yellow or orange solids in good yields (eq 3).



This synthetic route avoids the need to prepare the respective alkaline earth metal amides, $Ae\{N(SiMe_3)_2\}_2(THF)_n$, and permits the simple separation of products from the KI side-product by extraction into ether.

Compounds **2–4** are soluble in ethereal and aromatic solvents but only sparingly soluble in light petroleum and were purified by recrystallization from cold diethyl ether. The behavior of **2** contrasts with that of the homoleptic bis-(trimethylsilyl)phosphanides of the heavier alkaline earth metals $[Ae\{P(SiMe_3)_2\}_2]_2$, which are insoluble in toluene in the absence of coligands such as THF or DME [DME = 1,2-dimethoxyethane].²

With the exception of the cubane cluster complex $[Ca\{RPC_6H_4-2-O\}(THF)]_4 \cdot 4THF$,⁷ compounds **2–4** are the first examples of heavier alkaline earth phosphanides containing ligands in which the phosphorus atoms are not directly substituted by silyl groups. Additionally, compounds **1** and **2** represent the first crystallographically characterized examples of monomeric, homoleptic alkaline earth phosphanides; all previously reported alkaline earth bis-phosphanides adopt structural types I–IV in the solid state.

Solid-State Structures of 1–4. X-ray crystallography shows the homoleptic compounds **1** and **2** to be essentially isostructural but not isomorphous; compound **1** crystallizes with a molecule of THF in the unit cell. However, this solvent is only weakly held, and NMR spectra of samples of **1** which had been exposed to vacuum for 2 min show no evidence of THF. The molecular structures of **1** and **2** are shown in Figures 1 and 2, respectively, and details of bond lengths and angles are given in Table 2.

Compounds **1** and **2** are monomeric in the solid state, and the metal centers in each case are four-coordinate with a distorted tetrahedral geometry. Each phosphanide ligand binds the metal center through its N and P atoms to form two puckered six-membered chelate rings; the bite angles of the ligands are $90.89(6)^\circ$ and $89.93(6)^\circ$ for **1** and $84.27(4)^\circ$ and $83.29(4)^\circ$ for **2**, respectively, the larger bite angles observed in **1** being consistent with the greater ionic radius of Ca^{2+} than Mg^{2+} (1.00 and 0.72 Å, respectively, for a six-coordinate center).⁹ Remarkably, the remaining angles about the Mg and Ca atoms are very similar for the two compounds, illustrating the high degree of flexibility of the chelate ligands. Somewhat unexpectedly, given the steric

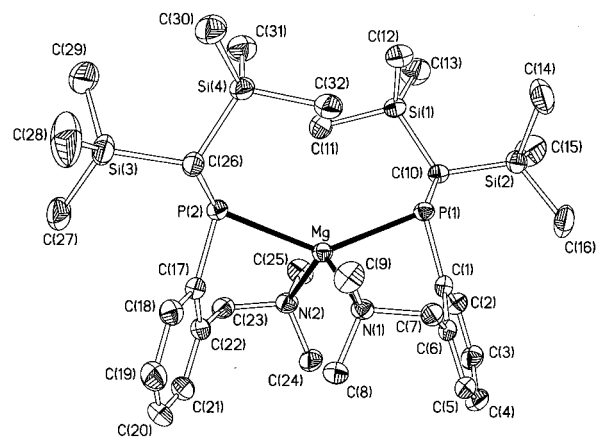


Figure 1. Molecular structure of **1** with 50% probability ellipsoids. H atoms and solvent THF omitted for clarity.

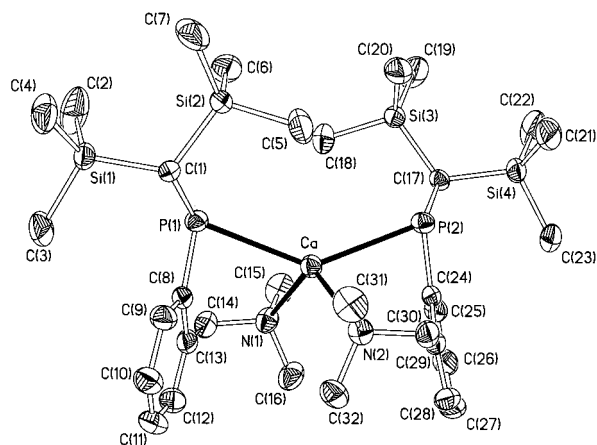


Figure 2. Molecular structure of **2** with 50% probability ellipsoids. H atoms omitted for clarity.

congestion about the Mg center, the Mg–P distances of 2.556(1) Å are similar to Mg–P distances in other magnesium phosphanides. For example, the Mg–P distances in the mononuclear complexes $Mg\{P(SiMe_3)_2\}_2(THF)_2$ and $Mg(PhPh)_2(tmeda)$ are 2.5031(6) Å, and 2.592(5) and 2.587(5) Å, respectively,^{3j,k} while the Mg–P distances in the trimeric complex $[\{(Me_3Si)_2P\}Mg\{\mu-P(SiMe_3)_2\}_2Mg]$ range from 2.451(2) to 2.678(2) Å.^{3d} In contrast, the Ca–P distances of 2.824(1) and 2.826(1) Å are the shortest such distances to be reported. For comparison, the Ca–P distances in the monomeric complexes $Ca\{P(SiMe_3)_2\}_2(THF)_4$ and $Ca\{P(SiMe_3)_2\}_2(TMTA)_2$ are 2.924(2) and 2.911(2) Å, and 2.994(2) Å, respectively [TMTA = 1,3,5-trimethyl-1,3,5-triazinane].^{3a,g} Although the Mg–N distances of 2.218(2) Å lie within the range typical for such distances, the Ca–N distances of 2.461(2) and 2.466(2) Å are the shortest reported distances between Ca and a tertiary amine center.^{2,10} The short Ca–P and Ca–N distances may be attributed to chelate ring formation and to the low coordination number of the calcium atom. That both **1** and **2** adopt the same structure in the solid state is somewhat surprising; the larger ionic radius of Ca^{2+} with respect to Mg^{2+} (1.00 and 0.72 Å, respectively)⁹

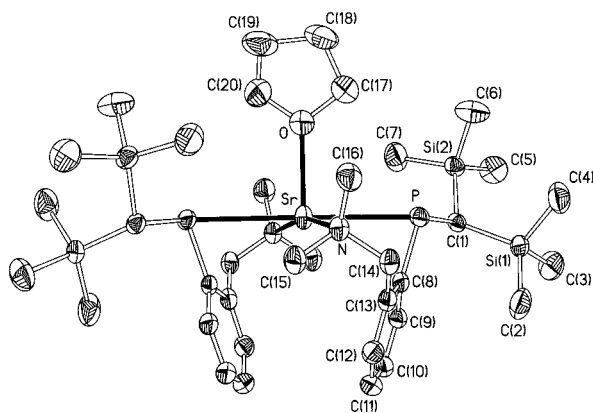
(10) A search of the Cambridge Crystallographic Database revealed no shorter distances between Ca and a tertiary amine: Allen, F. H.; Kennard, O. *Chem. Des. Autom. News* **1993**, 8, 31.

(11) Harvey, M. J.; Hanusa, T. P. *Organometallics* **2000**, 19, 1556.

(9) Shannon, R. D. *Acta Crystallogr., Sect. A* **1976**, A32, 751.

Table 2. Selected Bond Lengths (Å) and Angles (deg) for **1** and **2**

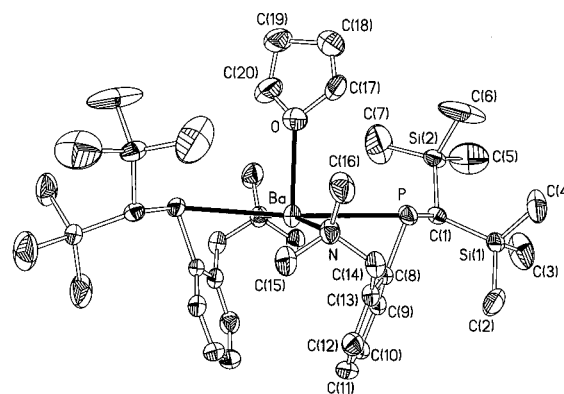
| | | | | 1 | |
|-----------------|------------|------------------|-------------|-------------|------------|
| Mg–N(1) | 2.218(2) | Mg–N(2) | 2.218(2) | Mg–P(1) | 2.5557(11) |
| Mg–P(2) | 2.5555(11) | P(1)–C(1) | 1.836(2) | P(2)–C(17) | 1.835(3) |
| P(1)–C(10) | 1.872(2) | P(2)–C(26) | 1.879(2) | C(10)–Si(1) | 1.892(2) |
| C(10)–Si(2) | 1.897(2) | C(26)–Si(3) | 1.902(2) | C(26)–Si(4) | 1.887(2) |
| N(1)–Mg–N(2) | 113.66(9) | P(1)–Mg–P(2) | 136.66(4) | | |
| P(1)–Mg–N(1) | 89.93(6) | P(2)–Mg–N(2) | 90.89(6) | | |
| N(1)–Mg–P(2) | 113.36(6) | N(2)–Mg–P(1) | 113.40(7) | | |
| Mg–P(1)–C(1) | 86.02(8) | Mg–P(2)–C(17) | 85.21(8) | | |
| Mg–P(1)–C(10) | 124.91(8) | Mg–P(2)–C(26) | 123.04(8) | | |
| C(1)–P(1)–C(10) | 103.81(11) | C(17)–P(2)–C(26) | 103.88(12) | | |
| | | | | 2 | |
| Ca–N(1) | 2.4661(16) | Ca–N(2) | 2.4613(15) | Ca–P(1) | 2.8258(6) |
| Ca–P(2) | 2.8239(6) | P(1)–C(8) | 1.8287(18) | P(2)–C(24) | 1.8256(18) |
| P(1)–C(1) | 1.8839(17) | P(2)–C(17) | 1.8877(16) | C(1)–Si(1) | 1.8800(17) |
| C(1)–Si(2) | 1.8759(17) | C(17)–Si(3) | 1.8775(18) | C(17)–Si(4) | 1.8819(17) |
| N(1)–Ca–N(2) | 112.39(5) | P(1)–Ca–P(2) | 137.768(18) | | |
| P(1)–Ca–N(1) | 83.29(4) | P(2)–Ca–N(2) | 84.27(4) | | |
| N(1)–Ca–P(2) | 119.67(4) | N(2)–Ca–P(1) | 121.51(4) | | |
| Ca–P(1)–C(8) | 80.39(6) | Ca–P(2)–C(24) | 79.87(5) | | |
| Ca–P(1)–C(1) | 121.80(5) | Ca–P(2)–C(17) | 124.65(6) | | |
| C(1)–P(1)–C(8) | 104.85(8) | C(17)–P(2)–C(24) | 105.32(8) | | |

**Figure 3.** Molecular structure of **3** with 50% probability ellipsoids. H atoms omitted for clarity.

would be expected to favor a higher coordination number for the former. The similarity between the structures of **1** and **2** may possibly be attributed to the flexible nature of the ligands, which are able to adjust considerably the internal angles about the phosphorus atoms in order to accommodate the different ionic radii of the metal ions (see later).

The monomeric compounds **3** and **4** are both isomorphous and isostructural in the solid state. The molecular structures of **3** and **4** are shown in Figures 3 and 4, respectively, and details of bond lengths and angles are given in Table 3.

The metal centers are each five-coordinate and adopt a distorted square pyramidal geometry with a crystallographic C_2 axis along the Sr/Ba–O vector. The phosphanide ligands bind through their N and P atoms to form the basal plane of the square pyramid and generate two puckered six-membered chelate rings with ligand bite angles of 75.31(4)° and 71.13(8)° for **3** and **4**, respectively. The coordination sphere of the metals in **3** and **4** is completed by a molecule of THF at the apex of the square pyramid. The gradual decrease in ligand bite angle from 90.89(6)° and 89.93(6)° in **1** to 71.13(8)° in **4** is consistent with the increasing ionic radii of the metal centers in **1–4**. In contrast to the corresponding

**Figure 4.** Molecular structure of **4** with 50% probability ellipsoids. H atoms omitted for clarity.**Table 3.** Selected Bond Lengths (Å) and Angles (deg) for **3** and **4**

| 3 | | | | | |
|----------------------|------------|-----------|------------|------------|----------|
| Sr–N | 2.6716(18) | Sr–P | 3.0902(6) | Sr–O | 2.517(3) |
| P–C(1) | 1.896(2) | P–C(8) | 1.833(2) | C(1)–Si(1) | 1.880(2) |
| C(1)–Si(2) | 1.878(2) | | | | |
| N–Sr–N' ^a | 164.38(3) | P–Sr–P' | 178.93(2) | | |
| P–Sr–N | 75.31(4) | N–Sr–P' | 104.54(4) | | |
| N–Sr–O | 97.81(4) | P–Sr–O | 90.534(12) | | |
| Sr–P–C(1) | 132.13(7) | Sr–P–C(8) | 72.43(6) | | |
| C(1)–P–C(8) | 103.65(9) | | | | |
| 4 | | | | | |
| Ba–N | 2.856(4) | Ba–P | 3.2719(13) | Ba–O | 2.701(7) |
| P–C(1) | 1.902(5) | P–C(8) | 1.828(5) | C(1)–Si(1) | 1.881(5) |
| C(1)–Si(2) | 1.869(5) | | | | |
| N–Ba–N' | 171.14(18) | P–Ba–P' | 175.46(5) | | |
| P–Ba–N | 71.13(8) | N–Ba–P' | 109.25(8) | | |
| N–Ba–O | 94.43(9) | P–Ba–O | 87.73(2) | | |
| Ba–P–C(1) | 122.73(15) | Ba–P–C(8) | 68.26(14) | | |
| C(1)–P–C(8) | 104.0(2) | | | | |

^a Symmetry operation for primed atoms $-x + 1, y, -z + 1/2$.

distances in **2**, the Sr–P and Ba–P distances of 3.090(1) and 3.272(1) Å, respectively, lie within the typical range for such bonds.³ For example, the Sr–P distances in Sr{P(SiMe₃)₂}₂(THF)₄ and Sr{P(SiMe₂Pr)₂}₂(THP)₄ are 3.035(6)

and 3.006(6) Å, and 3.0894(5) Å, respectively [THP = tetrahydropyran];^{3b,h} the Ba–P distances in Ba{P(SiMe₃)₂}-₂(THF)₄ and Ba{P(SiMe₂Prⁱ)₂}-₂(THF)₄ are 3.158(6) and 3.190(6) Å, and 3.200(1) and 3.184(1) Å, respectively.^{3c,g} The Sr–N and Ba–N distances also fall within the usual range for such distances.²

One of the more surprising features of **3** and **4** is the apparent low coordination numbers of the metal centers in view of their large ionic radii [according to Shannon, the ionic radii for six-coordinate Sr²⁺ and Ba²⁺ (the lowest coordination number for which data are available) are 1.18 and 1.35 Å, respectively].⁹ On first inspection, there appears to be a vacant coordination site beneath the AeN₂P₂ basal planes: the P–Ae–P' angles are 178.93(2)° and 175.46(5)°, and the N–Ae–N' angles are 164.38(8)° and 171.14(18)°, for **3** and **4**, respectively. However, the region beneath the basal plane of the square pyramid in both **3** and **4** is occupied by the aromatic rings of the phosphanide ligands, and these exhibit relatively short contacts between the *ipso*-carbon atoms adjacent to phosphorus and the metal centers in both cases. Unfortunately, there have been no previous reports of Sr···C_{ipso} interactions for direct comparison; however, the Sr···C(8) distance of 3.081(2) Å is somewhat longer than Sr–C distances in complexes where there is a strong Sr–C interaction. For example, the Sr–C distances in [{η⁵-C₅H₂-1,2,4-(SiMe₃)₃}Sr(μ-I)(THF)₂]₂ range from 2.856(7) to 2.878(6) Å and in {η⁵-C₅H₃-1,3-(SiMe₃)₂}Sr(THF) range from 2.78(4) to 2.84(5) Å.^{11,12} The Ba···C(8) distance of 3.101(4) Å is significantly shorter than the only previously reported example of this type of interaction [the Ba···C_{ipso} distances in Ba(η⁵-C₅Me₄SiMe₂Ph)₂ are 3.329(4) and 3.455(4) Å]¹³ but is longer than Ba–C distances in complexes in which there is a strong Ba–C interaction. For example, the Ba–C distances in (η⁵-C₅Me₅)₂BaL [L = 1,3,4,5-tetramethylimidazol-2-ylidene] are 2.989(9) and 2.985(15) Å (Ba–C(C₅-Me₅) average) and 2.951(3) Å (Ba–C(carbene));¹⁴ however, the Ba–C distances in [{η⁵-C₅H₂-1,2,4-(SiMe₃)₃}Ba(μ-I)(THF)₂]₂·^{1/2}C₇H₈ are similar to the Ba···C_{ipso} distance in **4** and range from 2.96(1) to 3.03(1) Å.¹¹ In both **3** and **4**, the phosphanide ligands are folded in toward the open face of the square pyramid such that the Sr–P–C(8) and Ba–P–C(8) angles are 72.43(6)° and 68.26(14)°, respectively. For comparison, the Ca–P–C_{ipso} angles in **2**, in which there are no short Ca···C_{ipso} contacts, are 79.87(5)° and 80.39(6)°. Thus, the Ae···C_{ipso} interactions in **3** and **4** appear to be genuine.

In compounds **1–4**, the phosphorus atoms adopt a pyramidal geometry, and the sum of angles about the P atoms increases as the ionic radii of the metals decrease, from 294.99° for **4** to 312.13° (average value) for **1**.

It is instructive to compare the structures of the alkaline earth metal compounds **1–4** with those of the previously

isolated divalent lanthanide analogues (THF)_nLn[PR(C₆H₄-2-CH₂NMe₂)₂]₂ [R = CH(SiMe₃)₂, Ln = Yb, n = 0 (**5**); Ln = Sm, n = 0 (**6**), 1 (**7**)].¹⁵ Both alkaline earth and lanthanide dications are hard acids which form essentially ionic metal–ligand interactions and which exhibit a pronounced oxophilicity; the ionic radii of Ca²⁺ and Yb²⁺ differ by 0.02 Å, while the ionic radii of Sr²⁺ and Sm²⁺ differ by just 0.01 Å.⁹

Although the available crystal structure data for the ytterbium complex **5** are poor,^{15a} preventing detailed comparisons, the complex appears to be essentially isostructural with the calcium complex **2**. Similarly, the strontium complex **3** is isomorphous and essentially isostructural with the THF-solvated samarium complex **7**: the Sr–P and Sm–P bond lengths are identical to within experimental error (Sr–P 3.090(1) Å, Sm–P 3.0873(8) Å), and the M–N and M–O distances are also similar (Sr–N 2.672(2), Sm–N 2.682(3) Å; Sr–O 2.517(3), Sm–O 2.535(3) Å). The internal angles about the Sr and Sm centers also show a strong correspondence; for example, the P–M–N ligand bite angles for **3** and **7** are 75.31(4)° and 75.01(6)°, respectively.^{15a}

Interestingly, similar M···C_{ipso} interactions are observed in **7** as are seen in **3** and **4**; the Sm···C(8) distance of 3.030(8) Å is remarkably similar to the Sr···C(8) distance in **3** [3.081(2) Å], and the Sm–P–C(8) angle of 70.89(8)° is also comparable with the Sr–P–C(8) angle in **3** [72.43(6)°]. No short contacts are found between the *ipso*-carbon atoms and the metal centers in the distorted tetrahedral, homoleptic complexes **1**, **2**, **5**, and **6**.

NMR Spectra and Solution Behavior of 1–4. At +85 °C, the ¹H NMR spectra of **2–4** in deuterated toluene are essentially consistent with their solid-state structures. A single set of signals due to the phosphanide ligands is observed in each case, although, even at this temperature, the signal due to the NMe₂ groups is extremely broad because of a dynamic exchange process. Single peaks are exhibited for the diastereotopic SiMe₃ groups for each complex at this temperature; this may be attributed to rapid, reversible P–Ae bond cleavage which is fast on the NMR time scale. A similar effect has been observed in the ytterbium(II) complex **5** and in alkali metal complexes of this ligand.^{8,15}

As the temperature is lowered, the signals due to the phosphanide ligands broaden and split to give very complex spectra indicative of the presence of more than one species in dynamic equilibrium. Unfortunately, even at the lowest temperature which we were able to obtain (–90 °C), these spectra consist of many broad, overlapping signals which do not sharpen sufficiently for detailed analysis.

The ³¹P{¹H} NMR spectra of **2–4** in toluene solution are more informative. The variable temperature spectra of these three compounds follow a similar pattern; hence, for simplicity, the following discussion will concentrate on the Sr complex **3**. At +52 °C, the spectrum consists of a single broad line at –60.4 ppm (A in Figure 5). As the temperature

(12) Engelhardt, L. M.; Junk, P. C.; Raston, C. L.; White, A. H. *Chem. Commun.* **1988**, 1500.

(13) Weeber, A.; Harder, S.; Brintzinger, H. H.; Knoll, K. *Organometallics* **2000**, *19*, 1325.

(14) Arduengo, A. J., III; Davidson, F.; Krafczyk, R.; Marshall, W. J.; Tamm, M. *Organometallics* **1998**, *17*, 3375.

(15) (a) Izod, K.; O'Shaughnessy, P.; Sheffield, J. M.; Clegg, W.; Liddle, S. T. *Inorg. Chem.* **2000**, *39*, 4741. (b) Clegg, W.; Izod, K.; Liddle, S. T. *J. Organomet. Chem.* **2000**, *613*, 128.

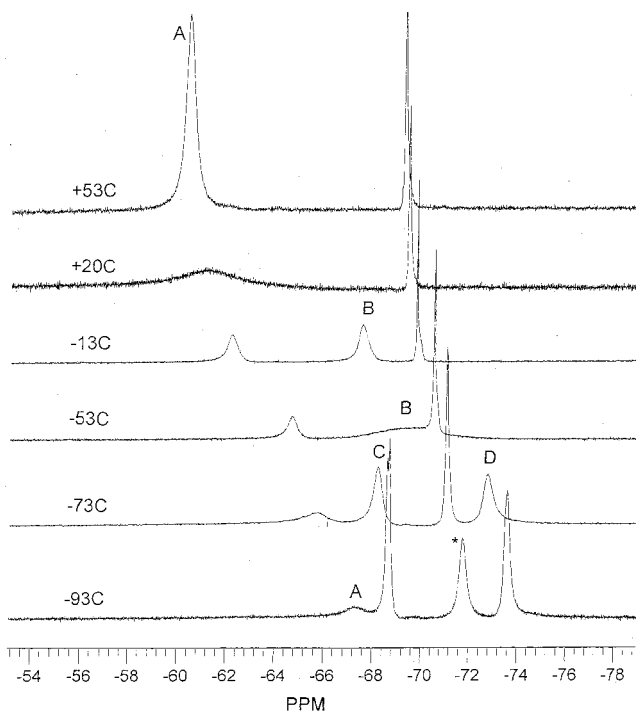


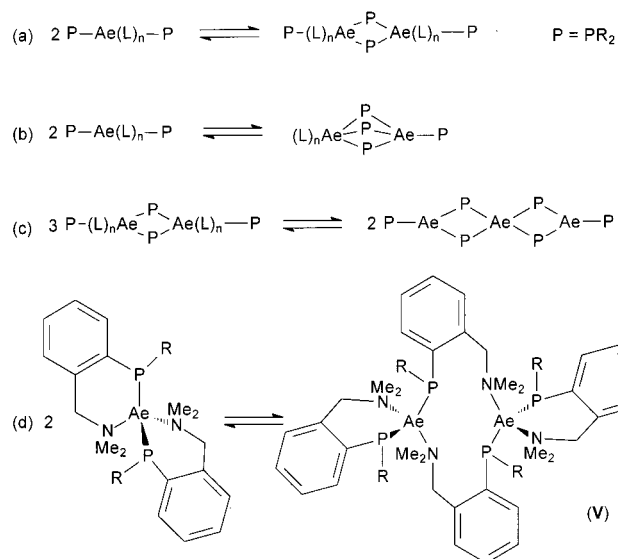
Figure 5. $^{31}\text{P}\{^1\text{H}\}$ NMR spectra of **3** in toluene solution between -93 and $+53$ °C. (Asterisk indicates free secondary phosphine due to partial hydrolysis.)

is reduced, this signal begins to broaden slightly until, at $+32$ °C, a new, very broad signal (B), centered at -65.1 ppm, begins to emerge. As the temperature is lowered further, signal B sharpens and increases in intensity at the expense of signal A. Below -33 °C, signal B broadens once again and at -63 °C splits into two signals of equal intensity at -68.3 and -72.7 ppm (C and D, respectively). These signals continue to sharpen and increase in intensity as the temperature is lowered still further, while signal A continues to decrease in intensity. At the lowest temperature that we were able to attain (-93 °C), signal C shows further splitting into two peaks while signal D exhibits a notable asymmetry. We attribute this to ^{31}P – ^{31}P coupling ($J_{\text{PP}} = 10.7$ Hz) which is resolved for C but not for D. At this temperature, integration of signals A, C, and D indicates that they are in the approximate ratio 1:6:6.

The variable temperature ^{31}P NMR spectra of the calcium and barium complexes **2** and **4** follow a similar pattern, the broad peak B appearing at -3 °C and -30 °C for **2** and **4**, respectively, and splitting into C and D at -53 °C (**2**) and -80 °C (**4**). Further splitting due to P–P coupling was not resolved in the spectra of **2** and **4** even at -90 °C. At this temperature, the ratio of peaks A, C, and D for **2** is approximately 1:3:3 (peaks A, C, and D overlap significantly in the spectrum of **4** at this temperature and are therefore not amenable to meaningful integration).

These spectra clearly indicate that **2**–**4** are subject to one or more dynamic processes in solution. We attribute this to a monomer–dimer equilibrium in which the monomer predominates at high temperatures. As the temperature is lowered, the concentration of the dimer (peak B) increases at the expense of that of the monomer (peak A). At lower

Scheme 1. (a–c) Dynamic Equilibria Exhibited by $\text{Ae}\{\text{P}(\text{SiR}_3)_2\}_2(\text{L})_n$ and (d) Dynamic Equilibrium Proposed for **1**



temperatures, signals due to the bridging and terminal phosphanide ligands in the dimer (peaks C and D) are resolved, and for **3** at the low-temperature limit, these appear to be part of an XY spin system. At higher temperatures, the bridging and terminal ligands undergo dynamic exchange for which the free energies of activation may be estimated as $\Delta G^\ddagger_{(232\text{K})} = 38.5$ kJ mol $^{-1}$ for **2** and $\Delta G^\ddagger_{(218\text{K})} = 40.9$ kJ mol $^{-1}$ for **3** from the coalescence temperatures (a sufficiently low temperature could not be obtained to completely freeze out this bridge–terminal exchange process for **4**, and hence, no value of ΔG^\ddagger could be obtained). Line shape analysis of the variable temperature ^{31}P NMR spectra of **2** yields $\Delta H^\ddagger = 31.6 \pm 3.0$ kJ mol $^{-1}$ and $\Delta S^\ddagger = -52 \pm 13$ J K $^{-1}$ mol $^{-1}$ for this bridge–terminal exchange, while for **3** $\Delta H^\ddagger = 35.7 \pm 2.7$ kJ mol $^{-1}$ and $\Delta S^\ddagger = -24 \pm 13$ J K $^{-1}$ mol $^{-1}$ for this process. Analysis of the concentrations of monomeric and dimeric species by careful integration of the relevant peaks in the ^{31}P NMR spectra yields $\Delta H = -21.4 \pm 5.0$ kJ mol $^{-1}$ and $\Delta S = -132 \pm 20$ J K $^{-1}$ mol $^{-1}$ for the monomer–dimer equilibrium in **2** and $\Delta H = -12.0 \pm 5.0$ kJ mol $^{-1}$ and $\Delta S = -38 \pm 20$ J K $^{-1}$ mol $^{-1}$ for the same process in **3**. The negative values of ΔS for this process are consistent with the predominance of the monomeric species at high temperatures.

Dynamic equilibria have been observed for a number of dimeric and trimeric alkaline earth metal phosphanides in nondonor solvents. The symmetrical complex $[(\text{THF})_2\{\text{Me}_2\text{-Pr}^i\text{Si}\}_2\text{P}\}\text{Ba}\{\mu\text{-P}(\text{SiMe}_2\text{Pr}^i)_2\}_2]$ (**8**) 3c and the unsymmetrical dimers $[(\text{THF})_3\text{Sr}\{\mu\text{-P}(\text{SiMe}_3)_2\}_3\text{Sr}\{\text{P}(\text{SiMe}_3)_2\}]$ (**9**) 3b and $[(\text{DME})_2\text{Ba}\{\mu\text{-P}(\text{SiMe}_2\text{CH}_2)_2\}_3\text{Ba}\{\text{P}(\text{SiMe}_2\text{CH}_2)_2\}(\text{DME})]$ (**10**) 3c are subject to monomer–dimer equilibria in toluene solution, although in each case it is the monomeric form which is favored at low temperatures (Scheme 1a,b). The predominance of the dimer at higher temperatures for **8**–**10** has been attributed to an entropic effect because dimerization is accompanied by elimination of neutral coligands. The homoleptic trimeric magnesium phosphanide $[\{\text{Me}_3\text{Si}\}_2\text{P}-$

$\text{Mg}\{\mu\text{-P}(\text{SiMe}_3)_2\}_2\text{Mg}\{\mu\text{-P}(\text{SiMe}_3)_2\}_2\text{Mg}\{\text{P}(\text{SiMe}_3)_2\}$ (**11**)^{3d} is subject to a dimer–trimer equilibrium in toluene solution in which the trimer is favored at low temperatures (Scheme 1c). Ab initio SCF calculations on the model complexes $\text{Ae}(\text{PH}_2)_2$ suggest that for $\text{Ae} = \text{Mg}$ the symmetrical dimeric form $(\text{PH}_2)\text{Mg}(\mu\text{-PH}_2)_2\text{Mg}(\text{PH}_2)$ is energetically favored, whereas for $\text{Ae} = \text{Ca}$ the unsymmetrical form $(\text{PH}_2)\text{Ca}(\mu\text{-PH}_2)_3\text{Ca}$ is favored.^{3f}

The solution behavior of **2–4** does not resemble that of **8–11**. In contrast to **8–10**, it is the dimeric form of **2–4** which predominates at low temperatures. Also, the low temperature ³¹P NMR spectra of **2–4** are not consistent with the presence of either a symmetrical dimer such as **8** or an unsymmetrical dimer such as **9** or **10**: the dimeric forms of **9** and **10** exhibit two signals in their ³¹P NMR spectra, a quartet and a doublet in the ratio 1:3, while the dimeric form of **8** should give rise to two triplets of equal intensity, although a temperature low enough to freeze out the bridge–terminal exchange could not be obtained for this complex and only a broad singlet was observed for the dimer. The low temperature ³¹P NMR spectra of the dimeric forms of **2–4** consist of two equal intensity signals which are partially resolved as doublets for **3**. This situation parallels that observed for the homoleptic ytterbium(II) complex **5** (which is isostructural with **2** in the solid state).^{15a} At $-88\text{ }^\circ\text{C}$, the ³¹P spectrum of **5** consists of a small peak due to the monomeric form (ca. 17%) along with a pair of equal intensity doublets [$J_{\text{PP}} = 19.0\text{ Hz}$ (cf. 10.7 Hz in **3**)] as the major signals (each signal exhibits additional satellites due to coupling to ¹⁷¹Yb). These latter signals have been interpreted as arising from a dimer in which each Yb center is chelated by one aminophosphanide ligand, while the other ligand bridges the two Yb atoms via its P and N centers in a head-to-tail fashion to give a structure of type V (Scheme 1d).

Thus, we suggest that the variable temperature ³¹P NMR spectra of **2–4** are consistent with a monomer–dimer equilibrium in which the dimeric form, which predominates at low temperatures, adopts a structure of type V. This structural type is unique in alkaline earth metal phosphanide chemistry.

In contrast, the ¹H, ¹³C, and ³¹P NMR spectra of complex **1** are sharp at or below room temperature. The room temperature proton NMR spectrum clearly shows the presence of a single ligand environment in which the diastereotopic $\text{C}(\text{SiMe}_3)_2$, NMe_2 , and CH_2N groups each appear as two separate signals. The two amino methyl groups are in very different environments and give rise to signals which are 1.33 ppm apart; the signals due to the benzylic protons are separated by 1.93 ppm. This clearly suggests that in **1** the six-membered chelate ring does not undergo dissociation over the measured temperature range, that is, Ae–P bond

cleavage is slow on the NMR time scale. This may be attributed to the high charge/radius ratio of Mg^{2+} and, hence, the presence of a stronger metal–ligand interaction. The ³¹P NMR spectrum of **1** shows no evidence for the formation of alternative oligomers even at $-90\text{ }^\circ\text{C}$; a single, sharp resonance at -99.3 ppm is observed at this temperature. It therefore appears that the greater Lewis acidity of the Mg^{2+} center stabilizes the monomeric form of **1** and disfavors the formation of dimeric species via the dissociative pathway necessary in the absence of donor solvents.

Interestingly, comparison of the room temperature ³¹P NMR data for **1–4** reveals a linear correlation between the ionic radius of the metal ion and the ³¹P chemical shift of the complex. A similar correlation has been observed for the ³¹P chemical shifts of the alkali metal phosphanides $\{(2,4,6\text{-Bu}^t_3\text{-C}_6\text{H}_2)\text{PH}\}\text{M}$ [$\text{M} = \text{Na–Cs}$] in $d_8\text{-THF}$.¹⁶

Conclusions

The combined steric and electronic properties of the potentially chelating aminophosphanide ligand $\{(\text{Me}_3\text{Si})_2\text{CH}\}\text{-P}(\text{C}_6\text{H}_4\text{-2-CH}_2\text{NMe}_2)^-$ enable the isolation of the first alkaline earth metal phosphanide complexes in which the ligand is not directly substituted by silyl groups. The bulky nature of the ligands also allows the isolation of complexes in which the alkaline earth metals have unusually low coordination numbers (e.g., complex **4** contains a formally five-coordinate Ba center).

Although monomeric in the solid state, complexes **2–4** are subject to dynamic processes in toluene solution that we ascribe to a monomer–dimer equilibrium in which the dimer is favored at low temperatures and for which, for **2** and **3**, exchange of the bridging and terminal phosphanide ligands may be frozen out at low temperatures. The low-temperature NMR spectra of **2–4** suggest that the dimer takes the form of a head-to-tail, P,N-bridged complex, a structural type which has not been observed previously in alkaline earth phosphanide complexes. In contrast, the magnesium complex **1** retains its monomeric form in toluene solution, even at temperatures as low as $-90\text{ }^\circ\text{C}$, and shows no evidence of dynamic behavior.

Acknowledgment. The authors thank Dr. M. N. S. Hill for obtaining the NMR spectra and for assistance with spectral simulations. This work was carried out with the support of the EPSRC and the Royal Society.

Supporting Information Available: X-ray crystallographic file in CIF format. This material is available free of charge via the Internet at <http://pubs.acs.org>.

IC0201194

(16) Rabe, G. W.; Heise, H.; Yap, G. P. A.; Liable-Sands, L. M.; Guzei, I. A.; Rheingold, A. L. *Inorg. Chem.* **1998**, *37*, 4235.